euspen's 26th International Conference & Exhibition, Krakow, PL, June 2026
www.euspen.eu

Simulation study on viscous friction reduction effect of textured oil-lubricated hydrostatic bearings

Dmytro Fedorynenko[1], Naofumi Ohnishi[1], and Yohichi Nakao[2]

[1] *Department of Aerospace Engineering, Tohoku University, Sendai, Japan*

[2] *Department of Mechanical Engineering, Kanagawa University, Yokohama, Japan* [1]

Correspondence: fedorynenko.dmytro.b3@tohoku.ac.jp

Abstract

In this study, the efficiency of a grinding spindle with textured oil-lubricated journal hydrostatic bearings was investigated via simulation. The bearing lubrication properties were defined using CFD simulations in ANSYS Fluent. A new approach for CFD analysis of textured hydrostatic bearings has been proposed, which simplifies the bearing fluid domain by dividing it into several subdomains with predefined boundary conditions. Then, the influence of rectangular-shaped micro-geometric patterns on oil velocity, pressure distribution, and power losses in the bearing-flowing parts was investigated for both streamwise and transverse groove orientations. The physical mechanism of friction reduction is identified as lid-driven cavity vortex formation within the grooves, which partially decouples the moving wall shear from the bulk lubricant flow. Transverse grooves on the moving wall achieve up to 48% wall shear stress reduction on circumferential lands, significantly outperforming streamwise grooves (~33%). The impact on bearing stiffness is assessed and shown to be minimal and can be fully recovered by restrictor re-optimization. It is demonstrated that applying specific texturing to bearing surfaces results in a decrease (approximately 30-48%) in the average wall shear stress and viscous friction losses without compromising bearing performance.

Keywords: textured bearing, hydrostatic bearing, grinding spindle, friction reduction, power consumption, CFD simulation, vortex

1. Introduction

Green tribology is a new research field that aims to achieve carbon neutrality. One constantly evolving direction in green tribology is improving bearing performance by reducing friction and achieving lower power consumption.

Hydrostatic bearings are precision mechanical components that utilize externally pressurized fluid films to support loads without metal-to-metal contacts. However, viscous shear in the lubricant film results in power losses that can significantly impact the overall efficiency of the system [1].

In recent years, micro-texturing has attracted considerable attention as an effective method for improving tribological performance [2-3]. By introducing controlled micro-scale features on bearing surfaces, it is possible to modify local fluid dynamics and reduce friction while maintaining, or even enhancing, load-carrying capacity (LCC).

However, there is currently no general explanation of how surface texturing affects spindle bearing performance in precision machining, where shaft eccentricity is small or close to zero. In this paper, the effects of micro-texturing of bearing surfaces on reducing viscous friction are considered for simplified flat regions that model the lands of a hydrostatic journal bearing. This study identifies the dominant friction reduction mechanism as lid-driven cavity vortex formation within the grooves, evaluates both streamwise and transverse groove orientations, and assesses the impact of texturing on bearing stiffness and load-carrying capacity to ensure that friction reduction does not compromise bearing performance.

2. Methodology

2.1. Computational Domain and Boundary Conditions

A typical hydrostatic bearing land surface can be divided into two areas as depicted in Fig. 1(a). The journal bearing has four recesses arranged symmetrically on the casing surface, separated by narrow lands. Figure 1(c) shows a 3D view of the journal surface; Figure 1(a) presents the corresponding developed (unfolded) view, where the cylindrical surface is mapped onto a plane with the circumferential direction running horizontally and the axial direction running vertically. Accordingly, the bearing computation domain representing the sliding part was modelled using two fluid subdomains, one for the circumferential land (fluid domain 1) and one for the axial land (fluid domain 2), shown in Fig. 1. In the simulations, flat squared regions are considered as bearing surfaces, as presented by colored parts in Fig. 1(a).

The value of recess pressure p_r was used as the pressure inlet and outlet conditions for the fluid domain 1 as shown in Fig. 1(b). For fluid domain 2, the inlet pressure was defined as p_r, and the pressure outlet value was set to 0 as boundary conditions.

2.2 Texture Configurations

Four micro-texturing configurations were analysed in this study, as detailed in Table 1, for the streamwise and transverse directions of texture as shown in Fig. 2. In the streamwise orientation (0°), grooves are aligned parallel to the shaft sliding direction; in the transverse orientation (90°), grooves are perpendicular to it. 16 possible combinations of the four configurations were analysed for the fluid domains 1 and 2 in the streamwise direction. The same approach was then applied to the transverse direction, yielding 32 structural combinations.

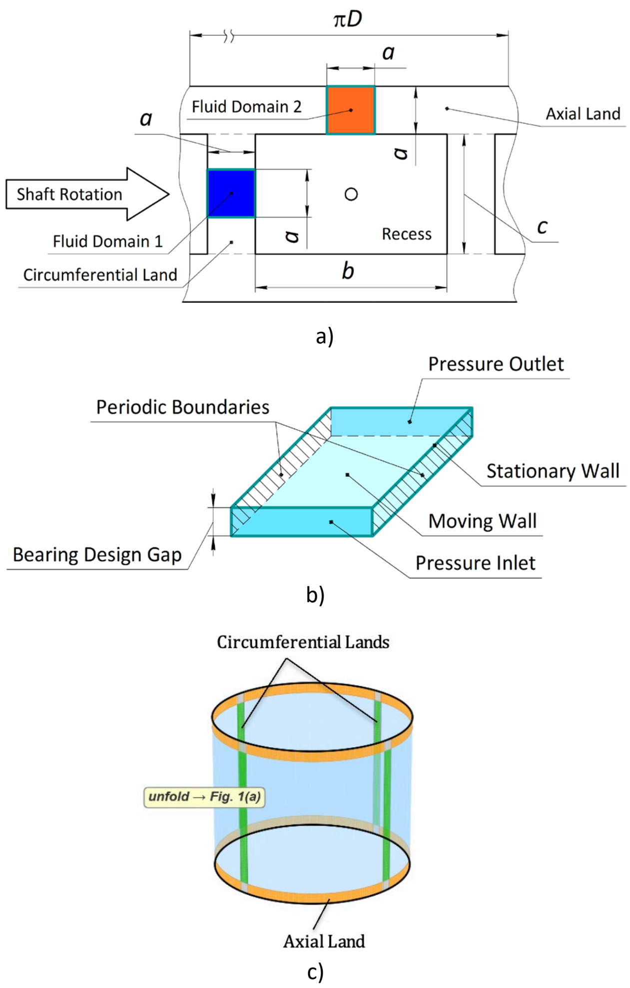

Figure 1. Bearing computation domains (a), boundary conditions (b), and (c) is 3D view of the journal bearing surface with four pockets (blue), circumferential lands (green), and axial lands (orange)

Table 1. Bearing surface configurations

Configuration	Stationary wall	Moving wall	Groove orientation
Smooth	smooth	smooth	-
Texture 1	textured	smooth	0°/90°
Texture 2	textured	textured	0°/90°
Texture 3	smooth	textured	0°/90°

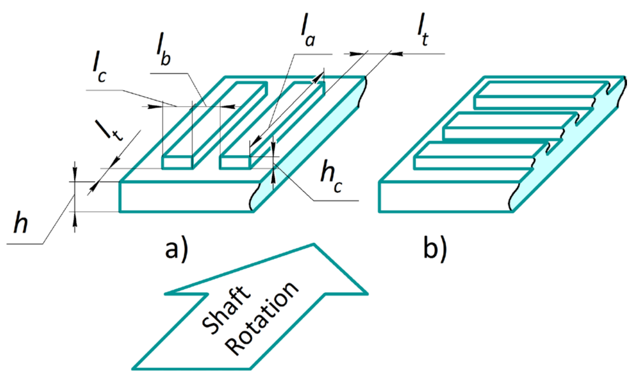

Figure 2. Fluid domain for streamwise (a) and transverse (b) directions of texture

The geometry of the transverse texture is identical to that of the streamwise texture, but rotated by 90°. In this study, the shaft rotation is aligned with the direction of the moving wall translational motion.

2.3 CFD Simulation Setup

Numerical simulations were performed using ANSYS Fluent with the following settings: steady-state, incompressible flow, no-slip boundary conditions at solid surfaces, and an isothermal assumption.

The thickness h of the bearing design gap was covered by 10 cells. The mesh resolution was refined near texture features using five boundary layers with a thickness of 0.5 µm each to capture flow gradients accurately. Grid independence was verified through mesh sensitivity studies.

The Reynolds number based on gap height is $Re = \rho U h/\eta$ = 51.5, confirming that the flow is well within the laminar regime ($Re \ll 2000$) and the steady-state assumption is valid. In the above formula ρ and η are the density and dynamic viscosity of fluid, respectively; U – journal sliding velocity. The groove-scale Reynolds number $Re\_groove = \rho U h_c/\eta$ = 20.6 is even smaller, ensuring that the cavity vortex remains laminar and steady. h_c denotes the groove depth (h_c =0.01 mm).

2.4 Performance Metrics

Total losses L in a journal hydrostatic bearing were defined as

$$L = \frac{p_s Q_m}{\rho} + U\left(\tau_{av} A_{sl} + n_r \frac{\eta A_r U}{h + h_r}\right), \quad (1)$$

where p_s – supply pressure; Q_m – mass flow rate through bearing axial lands; τ_{av} – area-averaged shear stress on the bearing circumferential and axial lands; A_{sl} and A_r – bearing lands area and recess area, respectively; n_r – number of recesses; h_r – recess depth.

The ratio of textured wall shear stress τ to smooth wall shear stress τ_s for Couette flow

$$\frac{\tau}{\tau_s} = \alpha(1-\varphi) + \frac{\varphi k h}{h + h_c}, \quad (2)$$

where α – inter-groove land shear correction factor, $\alpha = \tau_l/\tau_s$; τ_l – shear stress on flat inter-groove lands on a textured surface; φ – texture area ratio, $\varphi = l_c/(l_c + l_b)$; k – normalized vortex transmission factor representing the fraction of main-flow shear transmitted through the cavity vortex to the groove floor,

$$k = \frac{\tau_g}{\tau_l} \cdot \frac{h + h_c}{h},$$

τ_g – shear stress on the groove floor; l_c – groove width; l_b – width of the inter-groove land.

The groove aspect ratio A_g for a textured surface

$$A_g = \frac{l_c}{h_c}.$$

Pressure, velocity, wall shear stress distributions, and mass flow rate were derived using ANSYS Fluent simulation.

3. Results and Discussion

The main parameters of the tested simplified journal hydrostatic bearing model were as follows: p_s=2 MPa; p_r =1 Mpa; lubricant is oil VG5 with ρ=820 kg/m³ and η =0.007 Pa·s taken at 20°C; U =17.58 m/s; h =0.025 mm; recess depth h_r =3 mm; a=5 mm; b×c – 75×65 mm. The geometric sizes of the studied microtexture were taken as $l_c = l_b = h = 0.025$ mm; l_t =0.2 mm and l_a =4.6 mm.

Figure 3 presents the area-averaged wall shear stress and the total mass flow rate through two bearing axial lands for fluid domain 2 in the streamwise direction for all four cases.

All three textured configurations demonstrate significant friction reduction compared to the smooth reference. In particular, texture 2 yielded the greatest reduction in wall shear stress, approximately 38%; conversely, it exhibited the largest increase in mass flow rate, rising by 29%.

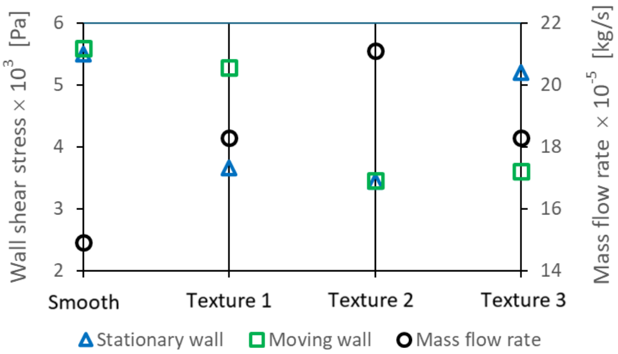

Figure 3. Comparison of wall shear stress and mass flow rate for fluid domain 2 in streamwise direction

Figure 4 shows the area-averaged wall shear stress for fluid domains 1 and 2 in the transverse direction for 3 cases.

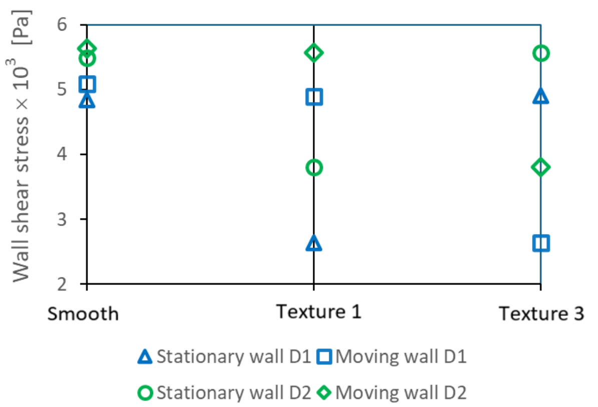

Figure 4. Comparison of wall shear stress for domain 1 (D1) and domain 2 (D2) in transverse direction

Notably, on the circumferential land (domain 1, pure Couette flow), transverse Texture 3 achieves a 48.3% wall shear stress reduction on the moving wall - significantly outperforming its streamwise counterpart (33.1%). This orientation dependence is a key finding discussed in Section 3.3.

3.2. Total Power Losses

Figure 5 illustrates power losses estimation for streamwise direction calculated using Eq. 1. It shows that Textures 2 and 3 achieved the highest reduction in total power losses for the streamwise orientation, lowering them by approximately 30% compared to the smooth case.

Figure 6 indicates total, pumping, and friction power losses, which are shown separately for domain 1 (D1) and domain 2 (D2) for the transverse direction. The transverse alignment of microgrooves on a moving wall (texture 3) achieves a 27.7% total loss reduction. This is because the circumferential lands (domain D1), which benefit most from transverse grooves, contribute significantly to total friction.

Combining transverse grooves on D1 with streamwise grooves on D2 yields the optimal result (Fig. 7): a 32.2% total loss reduction from 509 W to 345 W.

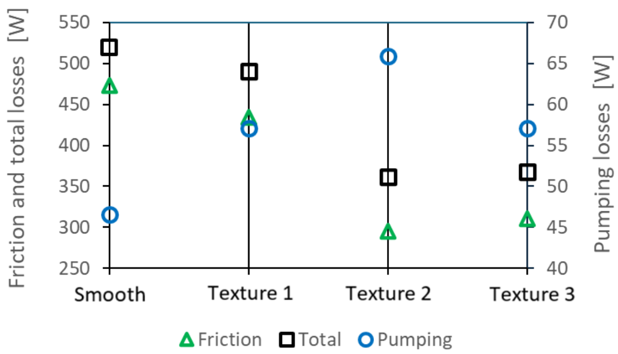

Figure 5. Power losses estimation for streamwise direction of texture

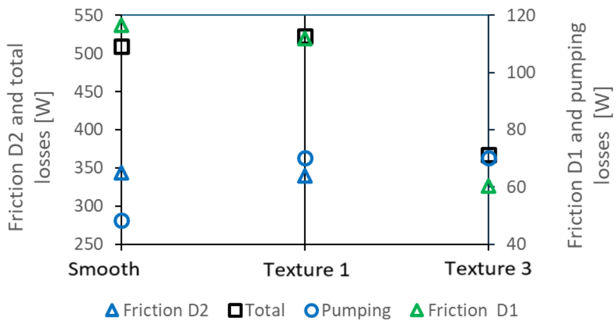

Figure 6. Power losses estimation for transverse direction of texture

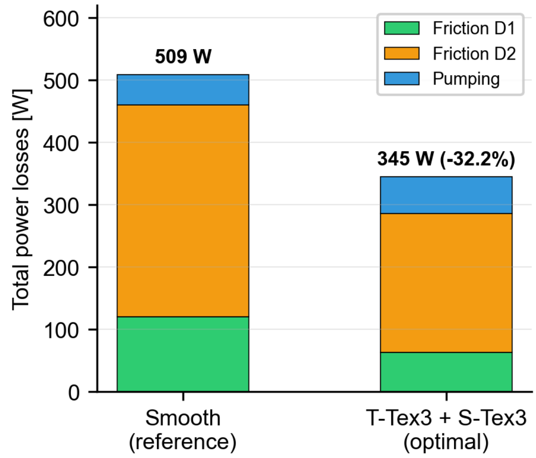

Figure 7. Full-bearing power losses: smooth reference vs optimal configuration (transverse Texture 3 on D1 + streamwise Texture 3 on D2)

3.3. Physical Mechanism of Friction Reduction

The physical mechanism underlying the observed friction reduction is depicted schematically in Fig. 8. When lubricant flows over a surface groove, the moving wall drags fluid into the cavity, generating a recirculating lid-driven vortex. This vortex partially decouples the high-velocity moving wall from the bulk flow in the bearing gap, effectively reducing the shear stress transmitted to the groove floor. Flow separation occurs at the leading edge and reattachment at the trailing edge of each groove, confining the recirculation within the cavity.

It was established that vortex factor k depends strongly on groove orientation, as summarised in Table 2. In the table, τ/τ_s (model) denotes the friction ratio predicted by the analytical formula given in Eq. 2, while τ/τ_s (CFD) is the ratio obtained directly from the CFD simulation results.

On the circumferential land (D1, pure Couette flow), transverse grooves achieve $k = 0.15$ versus $k = 0.33$ for streamwise, explaining the large orientation dependence observed in Section 3.1. The physical origin lies in the vortex topology: in transverse grooves, the main flow crosses the groove perpendicularly, generating a stable 2D recirculation whose axis is parallel to the groove length. This lid-driven cavity flow effectively seals the groove interior from the high-momentum main stream. In streamwise grooves, the flow enters the groove along its length, producing a weaker helical secondary flow that transmits more shear to the groove floor.

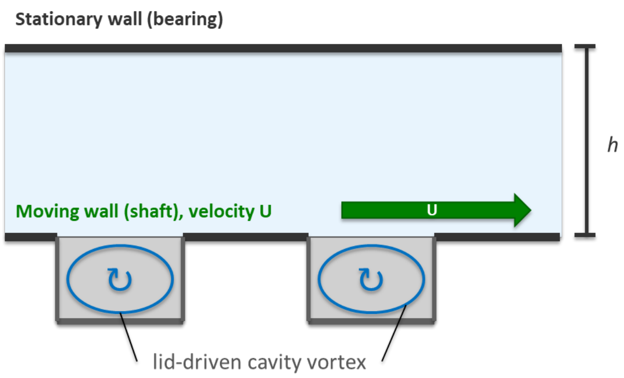

Figure 8. Groove cross-section schematic with lid-driven cavity vortex

Table 2. Vortex transmission factor k and friction reduction by orientation and domain

Orientation	Domain	k	τ/τ_s (model)	τ/τ_s (CFD)
Transverse	D1 (Couette)	0.15	0.52	0.52
Streamwise	D1 (Couette)	0.33	0.71	0.67
Transverse	D2 (Couette+ Poiseuille)	0.35	—	0.68
Streamwise	D2 (Couette+ Poiseuille)	0.33	—	0.64

On the axial land (D2), where Poiseuille flow coexists with Couette flow, the transverse advantage diminishes ($k \approx 0.35$) because the pressure-driven component is largely unaffected by transverse grooves. The groove aspect ratio $A_g = 2.5$ supports a single, well-defined vortex; for $A_g \ll 1$ multiple vortices may appear, while for $A_g \gg 1$ the vortex weakens, and direct shear increases k.

A critical concern is whether friction reduction compromises bearing stiffness or LCC. Surface texturing can increase the effective flow conductance of axial lands, leading to higher leakage flow rates. For a capillary-restricted hydrostatic bearing operating at the optimal restrictor ratio $\beta = 0.5$ [1], the stiffness K is proportional to $4\beta(1-\beta)$. When texturing increases the flow conductance by a factor r_Q, the restrictor ratio shifts to $\beta_{tex} = 1/(1+r_Q)$, affecting both LCC and stiffness. Table 3 summarizes these effects.

Table 3. Impact of texturing on bearing performance

Configuration (D1 + D2)	ΔQ_m [%]	ΔLCC [%]	ΔK [%]	ΔL [%]
Smooth + Smooth	0	0	0	reference
S-Tex3 + S-Tex3	+22.8	-10.2	-1.0	-28.7
T-Tex3 + Smooth	0	0	0	-11.1
T-Tex3 + S-Tex3	+22.8	-10.2	-1.0	-32.2
T-Tex3 + T-Tex3	+45.5	-18.5	-3.4	-27.7

Note: ΔQ_m – change in mass flow rate through D2 axial lands compared to the smooth reference; ΔLCC – change in load-carrying capacity; ΔK – change in bearing film stiffness; ΔL – change in total power losses; T and S – denote transverse and streamwise orientations, respectively.

Furthermore, the leakage increase caused by texturing can be compensated by re-optimizing the capillary restrictor. When texturing increases the bearing land conductance (lowering land resistance), the restrictor resistance must decrease by the same factor to restore $\beta = 0.5$. This requires increasing the capillary diameter. For example, for the optimal configuration (Tranverse-Texture 3 and Streamwise-Texture 3), the flow conductivity increases by $r_Q = 22.8\%$. The required increase in diameter is 5.3%. This simple geometric modification fully recovers the 10.2% LCC loss and restores bearing stiffness to its maximum value, while preserving the entire 32.2% friction reduction.

The cavity vortex dynamics that reduce friction are governed by local groove geometry and are independent of restrictor settings. Consequently, restrictor re-optimization and texture design can be treated as independent, sequential steps.

For precision spindles operating at near-zero eccentricity, uniform texturing across all lands preserves circumferential symmetry. This prevents the introduction of new error motion sources, ensuring that neither static stiffness nor dynamic precision is compromised.

4. Summary

This study evaluated the efficacy of micro-texturing in mitigating viscous friction within the hydrostatic journal bearings of precision grinding spindles using a simplified model. The analysis compares four distinct topologies: a smooth reference surface and three textured patterns varied by their orientation to the flow stream.

The physical mechanism of friction reduction was identified as lid-driven cavity vortex formation in the surface grooves. The vortex partially decouples the moving wall from the bulk lubricant, reducing the effective wall shear stress. The vortex transmission factor $k = 0.15$ for transverse grooves versus $k = 0.33$ for streamwise grooves explains the strong orientation dependence of friction reduction.

Among the tested patterns, transverse Texture 3 on circumferential lands combined with streamwise Texture 3 on axial lands achieves the optimal balance, reducing total power losses by 32.2% with only 1.0% stiffness reduction. After restrictor re-optimization, the LCC and stiffness losses can be fully recovered at zero cost to friction savings.

When balancing performance with manufacturing costs, Texture 3 emerges as the most suitable solution; it necessitates texturing of only the shaft journal surface while resulting in only 1.8% higher power losses than Texture 2.

Future work is planned to experimentally validate these findings and account for cavitation and viscous heating effects.

This research is supported by the Machine Tool Engineering Foundation and the Institute of Fluid Science of Tohoku University.

References

[1] Rowe W.B. 2012 Hydrostatic, aerostatic and hybrid bearing design. (Waltham: Butterworth-Heinemann Press).

[2] Etsion I. 2005 State of the art in laser surface texturing. J. Tribol. **127(1)** 248–253.

[3] Gropper D., Wang L., Harvey T.J. 2016 Hydrodynamic lubrication of textured surfaces: A review of modelling techniques and key findings. Tribol. Int. **94** 509–529.